Science of the Total Environment 700 (2020) 134464

Contents lists available at ScienceDirect

Science of the Total Environment

journal homepage: www.elsevier.com/locate/scitotenv

Influence of the seagrass *Thalassia hemprichii* on coral reef mesocosms exposed to ocean acidification and experimentally elevated temperatures

Pi-Jen Liu [a,b], Shin-Jing Ang [c], Anderson B. Mayfield [b,1], Hsing-Juh Lin [c,*]

[a] Graduate Institute of Marine Biology, National Dong-Hwa University, Pingtung 94450, Taiwan
[b] National Museum of Marine Biology and Aquarium, Pingtung 94450, Taiwan
[c] Department of Life Sciences and Innovation and Development Center of Sustainable Agriculture, National Chung Hsing University, Taichung 40227, Taiwan

HIGHLIGHTS

- The combined effect of OA and rising temperatures stimulated the growth of macroalgae.
- OA resulted in higher coral calcification rates when corals were co-incubated with seagrass.
- Macroalgal growth was lower in seagrass-containing mesocosms.
- Coral and macroalgal, but not seagrass, growth suffered at 31 °C under OA conditions.
- Seagrass helped to stabilize the system's metabolism in response to projected climate change stressors.

GRAPHICAL ABSTRACT

Conceptual model of climate change (ocean acidification [OA] and seawater warming) effects on coral reef mesocosms that either do (light blue) or do not (blue) feature seagrass beds. Solid lines denote abiotic effects (i.e., OA or OA + warming to 31C), whereas dotted lines depict effects of co-incubation with seagrass. CCM = carbon concentrating mechanism. ER=ecosystem respiration, GPP = gross primary production, NEP = net ecosystem metabolism, and P/R = photosynthesis/respiration ratio.

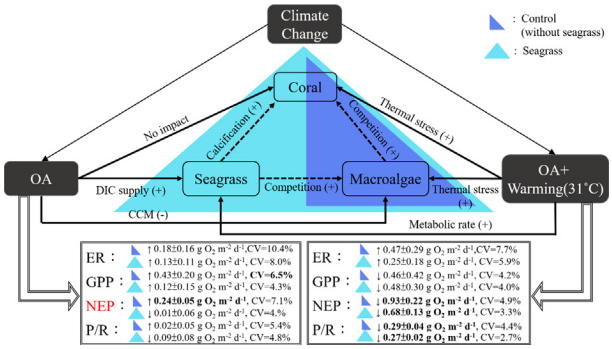

ARTICLE INFO

Article history:
Received 8 April 2019
Received in revised form 25 July 2019
Accepted 13 September 2019
Available online 4 October 2019

Keywords:
Climate change
Coral reefs
Ecosystem metabolism
Ecosystem production
Ocean acidification
Seagrass

ABSTRACT

Ocean acidification (OA) and warming currently threaten coastal ecosystems across the globe. However, it is possible that the former process could actually benefit marine plants, such as seagrasses. The purpose of this study was to examine whether the effects of the seagrass *Thalassia hemprichii* can increase the resilience of OA-challenged coral reef mesocosms whose temperatures were gradually elevated. It was found that seagrass shoot density, photosynthetic efficiency, and leaf growth rate actually increased with rising temperatures under OA. Macroalgal growth rates were higher in the seagrass-free mesocosms, but the calcification rate of the model reef coral *Pocillopora damicornis* was higher in coral reef mesocosms featuring seagrasses under OA at 25 and 28 °C. Both the macroalgal growth rate and the coral calcification rate decreased in all mesocosms when the temperature was raised to 31 °C under OA. However, the variation in gross primary production, ecosystem respiration, and net ecosystem production in the seagrass mesocosms was lower than in seagrass-free controls, suggesting that the presence of seagrass in the mesocosms helped to stabilize the metabolism of the system in response to simulated climate change.

* Corresponding author.
E-mail address: hjlin@dragon.nchu.edu.tw (H.-J. Lin).
[1] Present address: Atlantic Oceanographic and Meteorological Laboratory, National Oceanic and Atmospheric Administration, Miami, FL 33149, USA.

https://doi.org/10.1016/j.scitotenv.2019.134464
0048-9697/

1. Introduction

The CO_2 partial pressure (pCO_2) in the atmosphere reached 411 μatm in the summer of 2019 (https://www.esrl.noaa.gov/gmd/ccgg/trends/global.html), and representative concentration pathway (RCP) scenarios 2.6 (“controlled warming”) and 8.5 (“business as usual”) predict it to rise to 490 and 1370 μatm, respectively, by 2100 (van Vuuren et al., 2011). According to the IPCC’s “Coupled Model Intercomparison Project” (phase 5), the sea surface temperature (SST) will increase by 0.3–1.7 °C (RCP2.6) to 2.6–4.8 °C (RCP8.5) by 2081–2100 (Stocker et al., 2013). These temperature and pCO_2 increases will cause the ocean’s pH to decline by 0.13–0.42, resulting in ocean acidification (OA).

Since 1970, the ocean has absorbed approximately 93% of the additional heat due to global warming (Flato et al., 2013), leading to rising seawater temperatures. In general, when seawater temperatures rise above certain thermotolerance thresholds, species richness declines (Katsikatsou et al., 2012) and corals bleach (Diaz-Pulido et al., 2012). The differential responses of organisms to rising temperatures is expected to affect their interspecific interactions (Poloczanska et al., 2013). However, prior studies have tended to focus more on climate change-mediated effects on the distribution (Shalders et al., 2018) or physiology of individual species (Helmuth et al., 2013); the effect of rising temperatures on interspecific interactions is less commonly addressed (but see Lord et al., 2017, García et al., 2018).

With increasing pCO_2 (and declining pH), the concentration of HCO_3^- will increase relative to that of CO_3^{2-}, the latter being vital for the calcification of many marine organisms. The increase in HCO_3^- concentration, in contrast, is expected to stimulate the photosynthetic output of seagrasses and algae, which can use carbonic anhydrase to convert HCO_3^- to CO_2. Indeed, the productivity, shoot density, belowground biomass and carbon reserves of seagrasses have all been reported to increase in response to increased seawater pCO_2 (Palacios and Zimmerman, 2007, Andersson et al., 2011, Egea et al., 2018). The productivity and growth rate of non-calcareous algae also increased at pCO_2 levels ranging from 700 to 900 μatm (Porzio et al., 2011, Kroeker et al., 2013). However, the calcification rate of corals (Hoegh-Guldberg et al., 2007, Albright et al., 2016), sea urchins (Kurihara and Shirayama, 2004), shelled molluscs (Gazeau et al., 2013), and spider crabs (Walther et al., 2009) all decrease with increasing pCO_2, leading to weakened calcified structures.

Coral reefs are among the most biodiverse ecosystems on Earth and offer valuable ecosystem services to a plethora of organisms (as well as humankind; Knowlton, 2001; Costanza et al., 2014). However, over the past 20 years, phase shifts from coral- to macroalgal-dominated communities have occurred (Bellwood et al., 2004; Bruno and Valdivia, 2016). In 1980–1983, coral cover ranged from 20 to 50%, even reaching 100% on some reefs in the Indo-Pacific. However, it is uncommon to find reefs with >70% live coral cover today, with most less than 30% even 15 years ago (Bruno and Selig, 2007). Commensurate decreases in coral cover in the Caribbean have also been documented over the past 30 years: 50% in 1977 to 10% in 2002 (Gardner et al., 2003). Disease, overfishing, eutrophication, rising temperatures, and OA have all contributed to the demise of corals (Bruno and Valdivia, 2016), and the latter has been hypothesized to result in a shift from net calcium carbonate ($CaCO_3$) precipitating states to net dissolving ones (Baker et al., 2008). Furthermore, elevated temperatures are hypothesized to elicit bleaching events on an annual basis, which will result in dramatic community shifts given the wide variation in bleaching sensitivity across coral species (Donner et al., 2017).

Seagrasses are marine flowering plants that are widely distributed in shallow waters except in the Antarctic Ocean (den Hartog and Kuo, 2007). Seagrass beds are “blue carbon” sinks (Gillanders, 2007; Huang et al., 2015) that provide a number of ecosystem services, such as serving as food sources for mega-herbivores and as nursery grounds for a plethora of fish and invertebrates (Lee et al., 2015, 2016). Seagrasses are ecosystem engineers that can change the physical and chemical properties of seawater in a way that may affect nearby organisms, such as corals (van de Koppel et al., 2015). For example, the rhizomes of seagrasses can stabilize the sediments and filter seawater (Nordlund et al., 2017); the improved seawater clarity resulting from the latter process can lead to higher irradiance, which benefits the growth of corals and other photosynthetic organisms (Christianen et al., 2013).

Seagrasses and macroalgae can also absorb nutrients, which may suppress the growth of other macroalgae and/or seagrass in the near vicinity (Alexandre et al., 2017); however, others (Moreno-Marín et al., 2016) have shown that macroalgae can actually benefit the growth of seagrasses. As a specific example, both seagrasses and macroalgae can remove CO_2 and increase local pH and Ω_{Ar} of the surrounding seawater via their high photosynthetic rates (Lai et al., 2013); this East Asia finding has been observed elsewhere in the Pacific Ocean (Anthony et al., 2013), as well as in the Mediterranean (Hendriks et al., 2014) and the Caribbean (Manzello et al., 2012). Seagrass beds may consequently reduce the potential impact of OA on calcareous organisms (Keppel and Wardell-Johnson, 2012).

However, if both pCO_2 and temperature were to rise, it is less clear how seagrass beds may respond, nor do we know how coral reef + seagrass bed “mosaic habitats,” in which corals and seagrass-based communities overlap (prevalent in Southern Taiwan, as well as in the South China Sea; Lee et al., 2019) would be affected. Rising temperatures might impose detrimental impacts on seagrasses, and shallow intertidal seagrass beds are considered to be at the greatest risk (George et al., 2018); their relatively high respiration demands are expected to exceed their capacity for synthesizing organic carbon through photosynthesis upon prolonged exposure to elevated temperatures. Short-term high-temperature exposures, however, can actually stimulate seagrass autotrophy (Egea et al., 2019).

In this multi-factorial study, coral reef mesocosms in Southern Taiwan were cultured with and without seagrasses and exposed to both OA and gradually elevated temperatures. There were four questions aimed to be answered/addressed in this integrated mesocosm study: 1. Can seagrass increase the resilience of coral reef mesocosms under OA alone, as well as in response to OA plus elevated seawater temperatures? 2. How are net ecosystem calcification and production influenced by OA and elevated seawater temperatures? 3. Can seagrasses help calcifying macroalgae and corals resist elevated seawater temperatures under OA? 4. How do phytoplankton and benthic microalgae respond to elevated seawater temperatures under OA? Given the aforementioned ability of seagrasses to modify local pH, it was hypothesized that reef corals co-cultured with seagrasses would maintain higher growth rates under OA conditions than those corals cultured in the absence of seagrasses. We also hypothesized that elevated pCO_2 exposure, but not elevated temperatures, would enhance seagrass performance.

2. Materials and methods

2.1. Coral reef mesocosm facility

The coral reef mesocosm facility, which is located at the National Museum of Marine Biology and Aquarium (NMMBA), is approximately 10 km northwest of Taiwan’s Nanwan Bay

(21°57′N, 120°45′E). Six tanks (5.14 m^2 × 1 m depth; Fig. 1A) were designed to serve as models of the reefs of Nanwan Bay (Liu et al., 2009). The bottom of each tank was covered by a 3-cm layer of sand, and a few rocks were distributed across the benthos. A plastic plate (180 × 120 cm) was placed on the rocks, and two square baskets (81.5 × 81.5 × 6.5 cm [height]) covered with coral sand were placed on the sand to simulate a reef flat. There were two pumps in each tank: one was set up in the front side at 15 cm depth to produce wave simulations (1 Hz, 2–3 cm wave height, SE200, Wavemaker, Taiwan) and another was established along the back side to produce a disturbance current of flow-through seawater (250 W, 7200 L h^{-1}, Trundean, Taiwan). Sand-filtered seawater pumped directly from adjacent Houwan Bay (22°02′N, 120°41′E) was added to each tank at an exchange rate of 10% d^{-1} of the total volume.

Seawater temperature in each tank was initially maintained at 25.0 °C (±0.3 °C [SD for this and all other error terms in this section]) using a heat-exchanger (Great Helper System & XT130C, Dixell, Italy) to simulate the field temperature in the spring (Liu et al., 2009, 2015). During the experimental period, the photosynthetically active radiation (PAR) at 0.5-m tank depth was maintained at 258 ± 16.7 μmol photons m^{-2} s^{-1} from 0700 to 1700 hr (a 10:14-h light: dark photoperiod) by LED lamps (XLamp XT-E LEDs, Cree, Taiwan).

The biological components of these mesocosms were cultured at NMMBA for several years prior to the experiment, and a detailed list of the organisms added can be found in Table 1. There were some coral reef organisms already living in the tanks, including soft corals, sea anemones, hydroids, sponges, polychaetes, isopods, amphipods, symbiotic coral crabs, and macroalgae. At the location at which the wave maker was set up to simulate the reef crest, the corals *Montipora* sp., *Turbinaria* sp., *Fungia* sp., and *Millepora* sp. were deposited (Fig. 1B). On the front side of the "reef flat," the giant clam *Tridacna maxima* and the corals *Turbinaria* sp. and *Pavona cactus* were placed. The corals *Porites* sp., *Favia* sp., and *Heliopora coerulea* (blue coral) were deposited on the sand of each mesocosm, whereas nubbins were made from multiple colonies of the the model reef coral *Pocillopora damicornis* several weeks prior to experimentation (see timeline in Table 2.) and suspended on fishing line (9/mesocosm). Plants of the dominant seagrass species of Southern Taiwan, *Thalassia hemprichii*, were collected with a shovel (along with the sediment into which their roots permeated) from seagrass beds of Nanwan Bay. Approximately 3–4 seagrass shoots were transplanted to each of 324 flower pots (8.1 cm diameter × 6.7 cm depth), and each seagrass mesocosm (n = 3) received a total of 108 pots (equivalent to 681 ± 7 shoots m^{-2}) positioned within a 1.08 m^2 fenced-in enclosure to prevent grazing by sea urchins (Fig. 1C).

An Apex AquaController (USA) system (Supplementary Fig. 1) featuring the Apex base, the Energy Bar 8, the Apex display, a thermometer, a pH meter, and an ORP probe was used to control seawater temperature and pH; the latter was achieved by opening and closing a CO_2 tank (100%) connected to four tubes with free air stones at the end. The tubes were evenly distributed across each mesocosm to release CO_2, which quickly dissolved into the water. During OA treatments (described below), the release of CO_2 was initiated when the pH meter sensed a pH value >7.90 (10-min logging interval) and stopped when the pH value was <7.80; the target value sought to match the RCP6.0-projected pH of 7.85 (by the end of the 21st century). The total alkalinity (TA) remained relatively constant (2207 ± 45 μmol kg^{-1}) over the duration of the OA experiment (Supplementary Table 1), resulting in a pCO_2 of ~ 800 μatm at a pH of 7.85.

Three tanks featured seagrasses, while the other three were seagrass-free controls. The maximum, dark-adapted yield of photosystem II (Fv/Fm) of random seagrass shoots was assessed periodically (described in more detail below) after the shoots were transported from the ocean into the mesocosms in order to determine whether they had acclimated to their new environments (Supplementary Table 1). After 10 days of acclimation, the experiment began on 27 March 2017 (Table 2). Stage I was conducted for 14 days under a constant seawater temperature of 25 °C (the mean seawater temperature of Nanwan Bay in the spring); all tanks were maintained at ambient pCO_2 (~400 μatm), and we sought to document the effects of seagrass only in this stage. It was hypothesized that a 2-week duration would be sufficient to observe seagrass effects on corals given 1) prior work on coral + seagrass mosaic habitats in Southern Taiwan (Lin et al., 2018) and the South China Sea (Lee et al., 2019) and 2) the close proximity in which these fauna were cultured.

Stage II was conducted to examine the effect of OA (800 μatm) and seagrass presence for 28 days at 25 °C. A longer duration was chosen for this stage because the effects of OA on reef corals in particular have been found to be subtle (Comeau et al., 2014), or else not documented at all (Putnam et al., 2013) and so we hypothesized that more time would be required to elicit a detectable physiological response. Similarly, Stage III examined the combined effect of rising temperature (28 °C; the mean temperature of Nanwan Bay in the summer) and OA (800 μatm) for 28 days; since this "high" temperature is still well under the maximum experienced by coral reefs in Southern Taiwan (~30–30.5 °C in the summer; Mayfield et al., 2013), a longer duration was hypothesized to be needed to detect a shift in coral and/or seagrass behavior. Given that the SST is predicted to increase by 1.4–3.1 °C by the end of 21st century (RCP 6.0, Stocker et al., 2013), the seawater temperature was increased to 31 °C for 13 days at 800 μatm during Stage IV of the experiment. In contrast to Stages II and III, exposure to OA at 31 °C was hypothesized to elicit a stress response in the coral after only several days of treatment; therefore, the duration of this experimental stage was relatively short.

2.2. Biological response

The shoot density (shoots m^{-2}) of *T. hemprichii* was determined every two weeks by counting the number of shoots in each tank and dividing by the seagrass area (0.507 m^2). The leaf growth rate was also determined biweekly in each tank using the leaf marking method (Short and Duarte, 2001). Briefly, approximately five plants were randomly selected and marked in each tank at each measurement time. A small hole was punched through all of the leaves at the base of each shoot to provide a reference level. Approximately seven days after initial marking, the new growth increments of the leaves were measured. Using these measurements, the leaf growth rate was then expressed as mm $shoot^{-1}$ day^{-1}.

A submersible pulse amplitude-modulated (Diving-PAM) fluorometer (Waltz) was used to measure three fluorescence parameters from both coral nubbins (*P. damicornis*) and seagrass shoots (mentioned above): Fo (initial chlorophyll fluorescence after acclimating samples in darkness for 20 min when all reaction centers were open), Fm (maximum chlorophyll fluorescence after dark acclimation for 20 min when all reaction centers were closed following a saturating flash of light), and Fv/Fm (maximum quantum yield of photosystem II, where Fv = Fm-Fo). The calcification rate (mg $CaCO_3$ d^{-1}) of the coral *P. damicornis* was determined by the buoyant weighing technique (Davies, 1989), and mass increase per day was normalized to nubbin surface area using the modified wax dipping method, as modified by Mayfield et al. (2013).

Macroalgae began to proliferate rapidly in Stage II (OA). To assess algal growth, we scraped all algae off the plastic urchin exclusion screen (Fig. 1B-C; one side of the fence only) located close to the wave pump of each tank (size: 120 cm × 50 cm, but

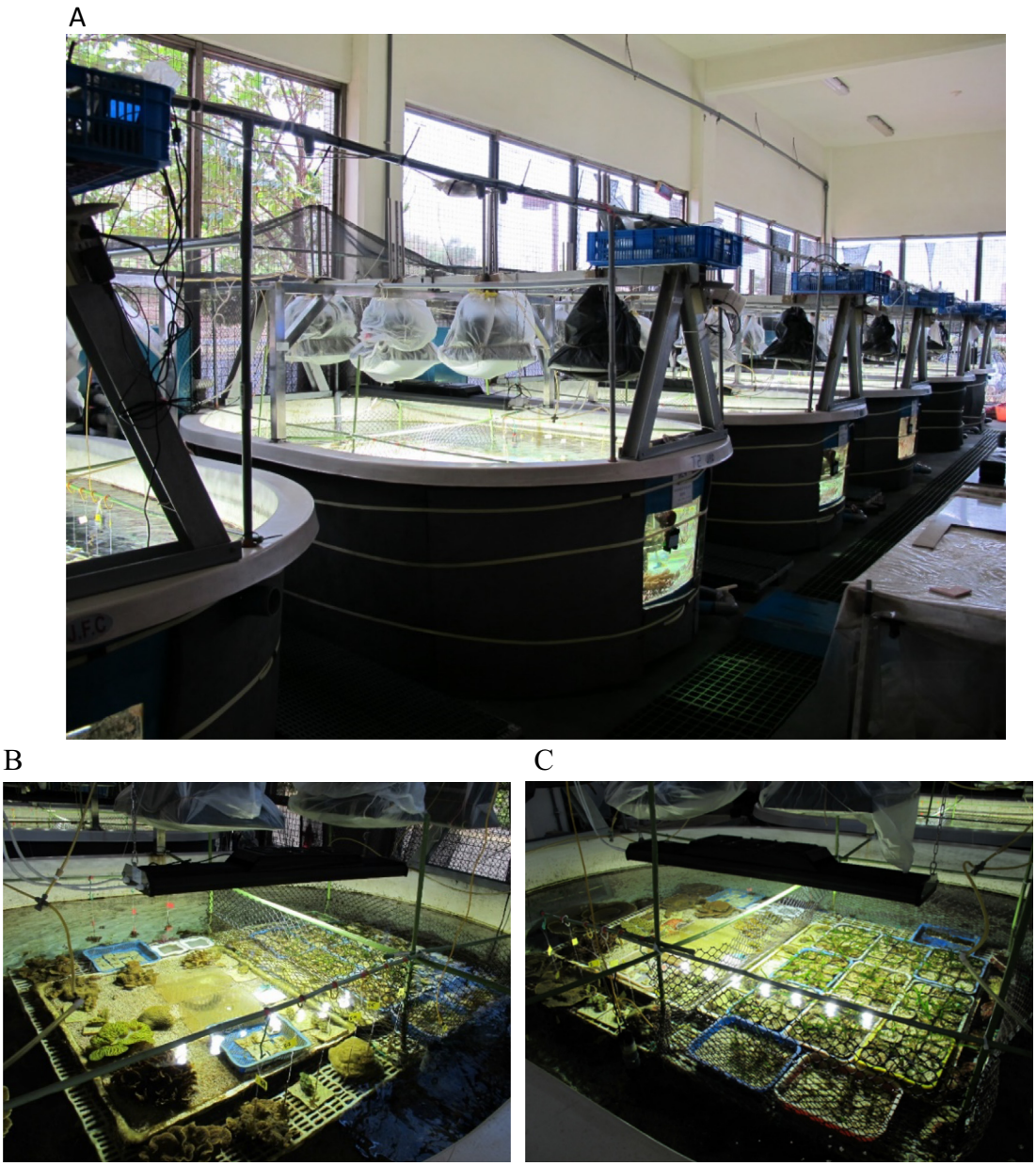

Fig. 1. (A) The coral reef mesocosm facility. (B) The front side of the mesocosm, which featured corals and giant clams, and (C) the rear side of the mesocosm, which housed the seagrasses. The black plastic mesh screen evident (~1 m^2) in (B)-(C) (between the front and rear sides) prevented seagrass grazing by sea urchins and served, additionally, as settlement material for macroalgae (see below for details.).

only 0.42 m^2 of underwater surface area) with a toothbrush. The plastic mesh was only briefly removed from each mesocosm before being returned to ensure that urchins did not graze seagrass blades during that time. The collected macroalgae were then weighed (wet weight), and the growth rate was determined by collecting all macroalgae that had accumulated each week in each tank, then normalizing to day (g wet weight d^{-1}).

Assessment of ecosystem metabolism can aid in understanding the interactions between organisms and their environments (Thorp and Delong, 2002; Marcarelli et al., 2011). Diel variation in dissolved oxygen (DO) concentration was used to determine the gross primary production (GPP), ecosystem respiration (ER), and net ecosystem metabolism (NEP) of each mesocosm herein (*sensu* Odum, 1956). A DO data logger (HOBO U-26, Onset, USA) was used to measure the changes in DO concentration (ΔDO; g O_2 m^{-2}) in each tank at a 30-minute logging interval over the duration of the experiment. In general, the ΔDO was driven by oxygen produced via photosynthesis during the day, the oxygen respired, and the air-seawater exchange of oxygen (Kemp and Boynton, 1980; see details below.). The ΔDO during the night was assumed to be driven by 1) respiration and 2) the air-seawater exchange of oxygen. Therefore, the hourly oxygen respiration rate during the night was calculated by correcting for the air-seawater exchange of oxygen and dividing by the time (hr). The air-sea exchange calculation followed Kemp and Boynton (1980): $(1-(DO_{sat,\ t2} + DO_{sat,\ t1})/200)*k*dt$, where $DO_{sat,\ t1}$ and $DO_{sat,\ t2}$ are the relative percent oxygen saturations (%) at times t1 and t2, respectively, k is the air-sea exchange coefficient, and dt is the time difference (in hours) between t2 and t1. DOTABLES (http://water.usgs.gov/software/DOTABLES/) was used to calculate oxygen saturations given the measured conditions in the tank. The wind and tide account for about the 50% of the total DO; therefore, when DO is 0, k is

Table 1
The number and total fresh weight (g) of the fish, mollusks, echinoderms, and corals present in the six mesocosms.

Taxon	Common name	Scientific name	Control mesocosms (without seagrass)			Seagrass mesocosms		
			T2	T4	T6	T1	T3	T5
Fish	Bowtie damselfish	*Neoglyphidodon melas*	2	1	2	2	2	2
	Blackspot sergeant	*Abudefduf sordidus*	0	1	0	0	0	0
	Silver moony	*Monodactylus argenteus*	8(15.7)	8(18.7)	8(21.7)	8(15.4)	8(13.2)	8(22.3)
	Eyestripe surgeonfish	*Acanthurus dussumieri*	1(550.8)	1(270.4)	1(394.6)	1(270.4)	1(349.9)	1(270.4)
	Two-tone tang	*Zebrasoma scopas*	1(8.5)	1(8.5)	1(8.5)	1(15.8)	1(13.0)	1(10.6)
	Jeweled blenny	*Salarias fasciatus*	3(24.0)	3(16.3)	3(27.6)	3(21.4)	3(20.1)	2(17.8)
	Decorated goby	*Istigobius decoratus*	1	1	1	1	1	1
Mollusks	Giant clam (large)	*Tridacna maxima*	2	2	1	2	1	1
	Giant clam (small)	*Tridacna maxima*	12	12	17	12	16	17
	Black-spotted topshell	*Trochus hanleyanus*	20(2 7 6)	20(2 8 4)	20(2 7 7)	20(2 8 5)	20(2 8 4)	20(2 7 4)
Echinoderms	Hawaiian sea urchin	*Tripneustes gratilla*	2(340)	2(339)	2(363)	2(358)	2(358)	2(335)
	Black sea cucumber	*Holothuria leucospilota*	5(1048)	5(1005)	5(1044)	5(1069)	5(1035)	4(1006)
Hydrozoans	Fire coral	*Millepora* sp.	1	1	1	1	1	1
Zoantharians	Cup coral	*Turbinaria* spp.	8	7	8	9	8	9
	Mushroom coral	Fungiidae	1	2	1	1	1	1
	Faviid coral	*Faviid* spp.	1	1	1	1	1	1
	Cactus coral	*Pavona cactus*	1	1	1	2	1	1
	Plating coral	*Montipora* sp.	1	3	3	1	1	1
	Massive coral	*Porites* spp.	1	1	1	2	1	1
	Cauliflower coral	*Pocillopora damicornis*	9	9	9	9	9	9
Alcyonarians	Blue coral	*Heliopora coerulea*	1	1	1	1	2	1

Table 2
The experimental design, including dates, duration, temperature, and pCO_2 of each experimental stage. Readers are referred to prior works for details on annual temperature variation in Nanwan Bay's coral reefs (Mayfield et al., 2012) and seagrass beds (Liu et al., 2012, Lin et al., 2018).

Stage	Duration	# days	Temperature (°C)	pCO_2 (μatm)
I	27 March-9 April 2017	14	25	400
II	10 April-7 May 2017	28	25	800
III	8 May-4 June 2017	28	28	800
IV	16 June-28 June 2017	13	31	800

assumed to be 0.5 g O_2 m^{-2} h^{-1} when estimating the sea-air exchange.

Assuming the hourly respiration rate during the night was similar to that of the day, the 24-hr (daily) respiration rate (also known as the ER rate) was calculated by multiplying the hourly night respiration rate by 24 hr. The GPP rate was then calculated by adding the ΔDO rate to the respiration rate during the day, and the NEP rate was calculated by deducting the ER rate from the GPP rate. These DO data were also used to calculate a GPP:ER (i.e., photosynthesis [P]:respiration [R]) ratio to serve as a system trophic index (*sensu* Odum, 1956).

2.3. Seawater quality data

The AquaController system automatically monitored water temperature and pH every 10 min. DO (mg L^{-1}) and salinity were monitored daily at 9:30 am in each tank using a portable "Professional Plus" meter from YSI (USA); DO was also measured more frequently by the approach described above. A HOBO® Pendant data logger (UA-002-64) was placed on the reef flat area of each mesocosm to measure underwater light and temperature at 30-min intervals during the experimental period. Light intensity (Lux) was transformed to photosynthetic photon flux density (PPFD) and expressed as μmol m^{-2} s^{-1} (Riddle, 2013).

Every week, seawater samples were collected from the middle layer (~0.5 m depth) of each tank for determination of TA(*sensu* Strickland and Parsons, 1972). TA, pH, seawater temperature, and salinity were then used to determine the pCO_2 and aragonite saturation state (Ω_{Ar}; *sensu* Lewis et al., 1998). Seawater samples were also collected from each tank at 10:00 am on a randomly selected day every week. These water samples were filtered through 0.45-μm filters (Pall Corporation) and then analyzed colorimetrically for concentrations of phosphate (Hach, USA), ammonium (Hach), nitrite (Pai and Riley, 1994), and nitrate (Pai and Riley, 1994).

2.4. Statistical analyses

Before statistical analyses, data were examined to determine whether residuals conformed to assumptions of normality and homogeneity of variance. If not, they were transformed (Clarke and Warwick, 2001) or analyzed using non-parametric statistical methods. After the mean value of each change was compared with the standard deviation, the slope (β) between the two was obtained by linear regression. When $\beta = 0$, no transformation was needed; when $\beta \geqq 0.5$ and $\geqq 0.75$, data were square and fourth root- transformed, respectively. If $\beta \geqq 1$, the data were log transformed. If the transformed data still did not meet the assumptions for parametrical statistical analyses, the appropriate non-parametric analysis was chosen according to the independence of the data. The four-stage experiment was separated into three parts (Table 2): Stage 1) effect of seagrass alone (25 °C and ambient pCO_2), Stage 2) the effect of seagrass presence under OA only, and Stages 3 and 4) the effect of seagrass presence under the combined effects of OA and warming to 28 °C and 31 °C, respectively. One-way repeated measures ANOVAs were used to determine the effect of OA (from Stage 1 to 2) or combined effects of OA and warming (from Stage 2 to 4) on seagrass responses. Two-way repeated-measures ANOVAs were applied to determine the effect of seagrass presence and OA only (from Stage 1 to 2) on seawater quality, other biological response variables (coral Fv/Fm,

coral calcification rate, and macroalgal growth rate), and system metabolism. Two-way repeated-measure ANOVAs were also carried out to determine the effect of seagrass presence and the combined effects of OA and warming (from Stage 2 to 4) on seawater quality, biological responses, and system metabolism. SigmaPlot 12.5 (SigmaStat, Systat Software GmbH, Germany) was used for the statistical analyses described above. Unless stated otherwise, all error terms presented below represent standard error (SE) of the mean, and an alpha level of 0.05 was established *a priori*.

3. Results

3.1. Seawater quality response to OA and rising temperatures

In Stages I and II, the effect of OA alone on seawater quality was more pronounced than the effect of seagrass presence (Table 3). For all mesocosms, the pH was effectively dropped to its target value of ~7.85, and DO concentration decreased in concert (Supplementary Table 2). There were no significant differences in pCO_2, DIC concentration, Ω_{Ar}, and TA between the seagrass mesocosms and the controls; upon OA alone in Stage II, pCO_2 and DIC concentration in all mesocosms increased 91 and 6%, respectively (Table 3). However, Ω_{Ar} decreased 37% upon acidifying the seawater. OA did not affect TA, but it did result in significant changes in concentrations of various seawater carbon species in all mesocosms (Supplementary Table 2). The concentrations of HCO_3^- and CO_2 increased 10 and 85%, respectively, in response to OA alone in Stage II, whereas the concentration of CO_3^{2-} decreased by 37%.

All mesocosms were oligotrophic in Stage I (Table 3). After OA alone (Stage II), the phosphate concentration increased 18% in the seagrass mesocosms though decreased 73% in the controls. The concentrations of ammonium, nitrite, and nitrate increased 95, 55, and 61%, respectively, after OA alone (Supplementary Table 2). While seawater temperature was programmed to increase from stage II (25 °C) to stage IV (31 °C), DO decreased only 4% over this period (Table 3). There were significant differences in seawater carbon species concentrations in response to the combined effect of OA and warming for all mesocosms (Supplementary Table 3). The concentrations of both pCO_2 and CO_2 were slightly higher (7 and 8%, respectively) in all mesocosms at 28 °C than at 25 °C and 31 °C (Table 3). Rising temperatures slightly reduced TA and Ω_{Ar}, as well as the concentrations of DIC, HCO_3^-, and CO_3^{2-} for all mesocosms. TA, Ω_{Ar}, DIC, and concentrations of HCO_3^- and CO_3^{2-} decreased 3, 8, 2, 2, and 9%, respectively, from 25 °C to 31 °C.

The combined effect of OA and warming resulted in a significantly higher phosphate concentration in the seagrass mesocosms than in the controls (Supplementary Table 3). The concentrations of nitrite and nitrate in all mesocosms at 31 °C were 1.22 and 3.49-fold higher, respectively, than at 25 °C and 28 °C (Table 3). The concentrations of nitrite and nitrate in the seagrass mesocosms tended to be higher (35 and 72%, respectively) than in the controls at higher temperatures under OA, though the differences were only marginally significant (Supplementary Table 3).

3.2. Seagrass response to OA and rising temperatures

OA led to a significant increase in both *T. hemprichii* shoot density (Fig. 2A) and leaf growth rate (Fig. 2B) at 25 °C (Stage II): increasing 4 and 25%, respectively (Supplementary Table 4). In contrast, Fv/Fm decreased slightly from 0.813 ± 0.003 (Stage I) to 0.799 ± 0.005 upon OA treatment (Stage II), though later recovered (even as temperatures rose; Fig. 2C). Further rising of the temperature (Stage II to Stages III and IV) also led to significant increases in shoot density (18%) and leaf growth rate (35%) at 31 °C (Supplementary Table 5). Fv/Fm also increased to 0.822 ± 0.004 at 31 °C.

3.3. Macroalgal response to OA and rising temperatures

OA and rising temperatures stimulated the growth of macroalgae (Fig. 3); after OA, the macroalga *Dictyota bartayresiana* started to grow rapidly in all mesocosms (Supplementary Fig. 2), and its growth rate was 2-fold higher in the controls than in the seagrass mesocosms at 25 °C and 28 °C. However, its growth slowed at 31 °C in all mesocosms (Fig. 3).

3.4. Coral response to OA and rising temperatures

OA did not significantly affect coral Fv/Fm, which ranged from 0.737 to 0.750 (Fig. 4A). However, coral Fv/Fm decreased gradually with rising temperatures under OA conditions for all mesocosms. There was no significant difference in coral Fv/Fm between the seagrass mesocosms and the controls (Supplementary Tables 6 and 7). The coral calcification rate was significantly higher in the seagrass mesocosms than in the controls at 25 °C and 28 °C under OA (Fig. 4B). However, the coral calcification rate was significantly lower at 31 °C + OA for all mesocosms (Supplementary Table 7).

3.5. System metabolic response to OA and rising temperatures

In Stages I and II, there were no significant differences in the ER rates between the control and seagrass mesocosms (Supplementary Table 6). For all mesocosms, the ER increased gradually with rising temperatures from Stage II to IV under OA conditions (Fig. 5A). Moreover, the ER was significantly higher in the controls than in the seagrass mesocosms at 28 °C and 31 °C under OA (Supplementary Table 7). In Stages I and II, there was no significant difference in the GPP between the control and seagrass mesocosms, nor did OA affect GPP (Supplementary Table 6). However, the GPP in all mesocosms increased from the lowest values at 25 °C to the highest values at 28 °C (Fig. 5B). GPP was similar at 28 °C and 31 °C. The GPP was also significantly higher in the controls than in the seagrass mesocosms when pooling the data across all sampling times from Stage II to IV (Supplementary Table 7).

In Stage II, OA did not affect the NEP in the seagrass mesocosms (Fig. 5C). However, the NEP in the controls increased significantly after OA (Supplementary Table 6). The NEP in all mesocosms decreased significantly with rising temperatures and reached the lowest value at 31 °C under OA (Supplementary Table 7). The NEP in the seagrass mesocosms tended to be lower than in the controls for all temperature treatments (Fig. 5C), though no significant difference was detected.

In Stage II, the P:R ratio was not affected by OA alone (Fig. 5D). However, rising temperatures significantly decreased the P:R ratio in all mesocosms, and lowest values were measured at 31 °C under OA (Supplementary Tables 6 and 7). No significant difference in the P:R ratio was detected between the control and seagrass mesocosms.

4. Discussion

Effects of OA on different primary producers. Upon pumping CO_2 into the seawater, all mesocosms underwent increases in the concentrations of H_2CO_3, HCO_3^-, and H^+; the CO_3^{2-} concentration and pH both decreased, as was hypothesized. Importantly, the concentration of HCO_3^- was higher than CO_2. Since the $K_{0.5}$ of CO_2 is 2–3 times lower than that of HCO_3^-, CO_2 is the preferred carbon source for seagrasses and macroalgae (Sand-Jensen and Gordon, 1984). However, due to the slow dispersion rate and low concentration of CO_2 in seawater, most marine producers are C_3 plants and use HCO_3^- as their primary carbon source (Koch et al., 2013). Particularly, the lower utilization efficiency of HCO_3^- by seagrasses than

Table 3
Seawater quality (mean ± SE; n = 3) in the four stages of the experiment in both seagrass and control (i.e., seagrass-free) mesocosms.

	25 °C (ambient pCO_2)		25 °C (acidification)		28 °C (acidification)		31 °C (acidification)	
	Control	Seagrass	Control	Seagrass	Control	Seagrass	Control	Seagrass
pH	8.06 ± 0.01	8.10 ± 0.04	7.86 ± 0.00	7.86 ± 0.01	7.85 ± 0.00	7.86 ± 0.01	7.85 ± 0.00	7.86 ± 0.00
Temperature (°C)	25.0 ± 0.0	25.0 ± 0.1	25.1 ± 0.0	25.1 ± 0.1	27.9 ± 0.0	27.9 ± 0.0	30.8 ± 0.1	30.8 ± 0.0
Photosynthetically active radiation (PAR, μmol m^{-2} s^{-1})	274.0 ± 2.4	267.7 ± 10.8	242.0 ± 20.4	281.4 ± 9.5	256.1 ± 13.6	248.7 ± 20.0	251.2 ± 14.1	247.4 ± 33.3
DO (mg L^{-1})	6.84 ± 0.00	6.84 ± 0.01	6.78 ± 0.00	6.79 ± 0.01	6.49 ± 0.00	6.49 ± 0.00	6.24 ± 0.00	6.24 ± 0.00
Salinity	35.07 ± 0.06	35.09 ± 0.04	34.99 ± 0.01	35.03 ± 0.01	34.67 ± 0.07	34.77 ± 0.04	33.80 ± 0.10	33.86 ± 0.06
pCO_2 (μatm)	449 ± 4	418 ± 20	818 ± 7	837 ± 19	891 ± 12	906 ± 13	853 ± 21	825 ± 10
TA (μmol kg^{-1})	2093 ± 10	2157 ± 25	2114 ± 22	2148 ± 42	2090 ± 2	2096 ± 32	2073 ± 15	2066 ± 19
Ω_{Ar}	2.72 ± 0.02	2.99 ± 0.15	1.78 ± 0.02	1.80 ± 0.05	1.61 ± 0.02	1.60 ± 0.03	1.64 ± 0.03	1.67 ± 0.04
DIC (μmol kg^{-1})	1849 ± 9	1889 ± 13	1971 ± 21	2004 ± 39	1963 ± 3	1971 ± 30	1945 ± 15	1934 ± 15
HCO_3^- (μmol kg^{-1})	1665 ± 8	1689 ± 8	1836 ± 19	1867 ± 36	1837 ± 4	1844 ± 28	1819 ± 15	1807 ± 12
CO_3^{2-} (μmol kg^{-1})	171 ± 1	188 ± 9	112 ± 2	113 ± 3	101 ± 1	101 ± 2	102 ± 2	104 ± 3
CO_2 (μmol kg^{-1})	13 ± 0	12 ± 1	23 ± 0	24 ± 1	25 ± 0	26 ± 0	24 ± 1	23 ± 0
PO_4^{3-} (μmol L^{-1})	0.085 ± 0.027	0.117 ± 0.045	0.034 ± 0.010	0.142 ± 0.067	0.058 ± 0.016	0.082 ± 0.018	0.079 ± 0.042	0.158 ± 0.073
NH_4^+ (μmol L^{-1})	0.520 ± 0.044	0.621 ± 0.120	0.958 ± 0.035	1.215 ± 0.113	0.757 ± 0.054	0.879 ± 0.015	0.924 ± 0.136	1.007 ± 0.170
NO_2^- (μmol L^{-1})	0.086 ± 0.012	0.099 ± 0.023	0.125 ± 0.012	0.172 ± 0.007	0.141 ± 0.015	0.154 ± 0.019	0.246 ± 0.044	0.402 ± 0.044
NO_3^- (μmol L^{-1})	0.262 ± 0.040	0.576 ± 0.287	0.466 ± 0.029	0.889 ± 0.256	0.229 ± 0.094	1.142 ± 0.269	1.204 ± 0.190	4.922 ± 1.765

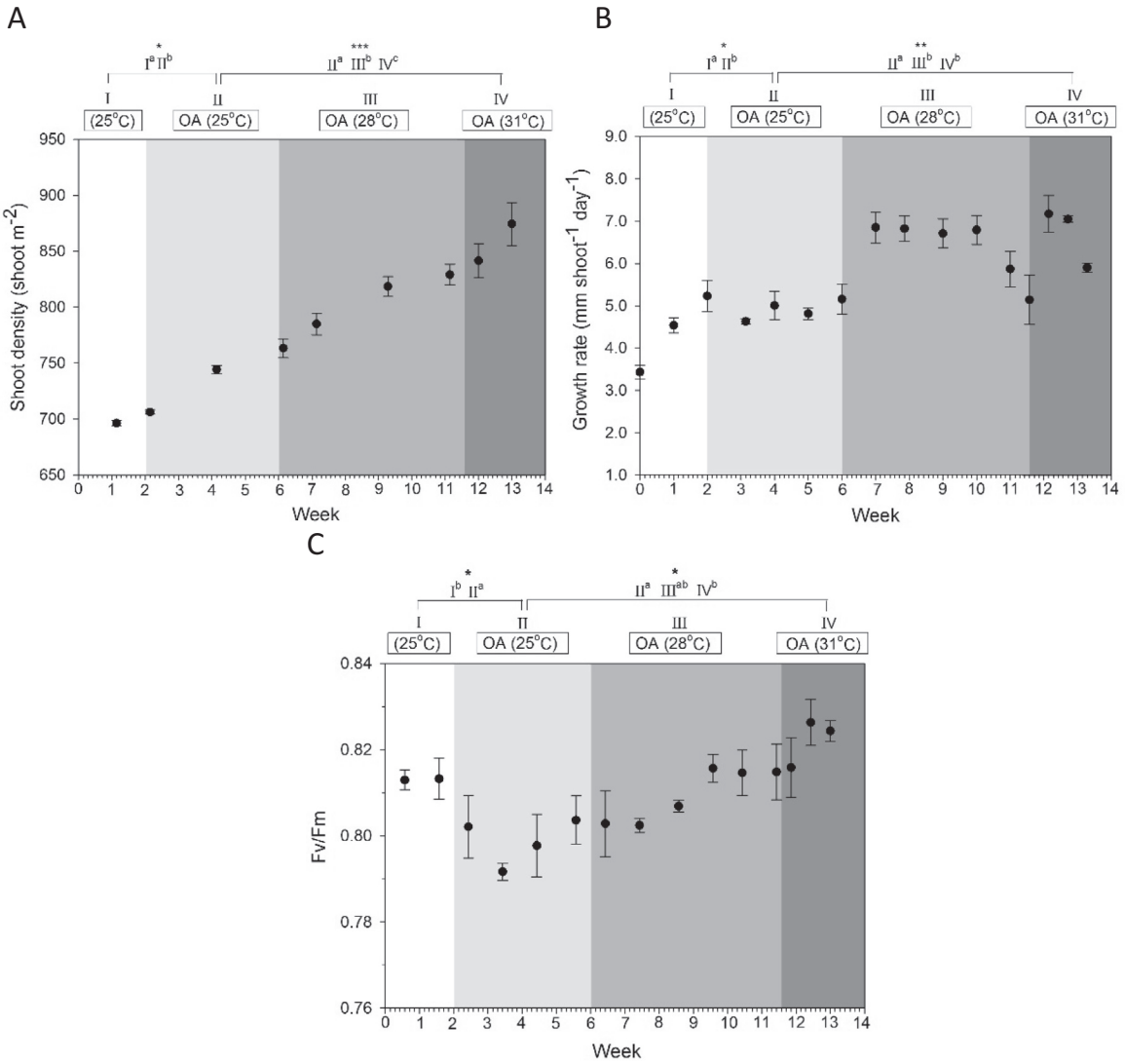

Fig. 2. Seagrass (A) shoot density, (B) leaf growth rate, and (C) maximum quantum yield of photosystem II (Fv/Fm) across the four stages (denoted by shading) of the experiment (mean ± SE; n = 3). Lowercase letters adjacent to experimental stage at the top of each panel signify significant differences (Tukey's $p < 0.05$) between the means for each experimental stage, as repeated measures ANOVAs detected significant overall effects of ocean acidification [OA] (from Stage I to II) and combined effects of OA and warming (from Stage II to IV) for each response variable (Supplementary Tables 4 and 5)(T). In all cases, the group labeled "a" possessed the lowest value of the respective response variable.

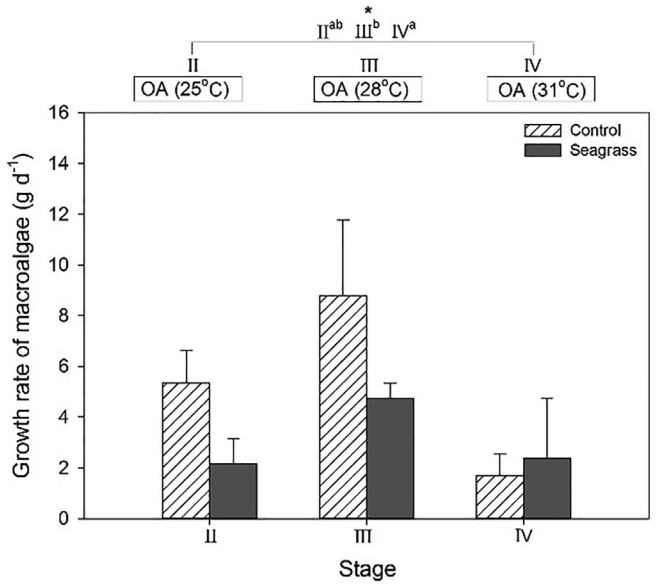

Fig. 3. The growth rate of macroalgae in control and seagrass mesocosms (mean ± SE; n = 3) for the latter three stages of the experiment. No macroalgae were observed during Stage I (prior to ocean acidification [OA]). Lowercase letters at the top of the figure signify significant differences (Tukey's $p < 0.05$) across stages.

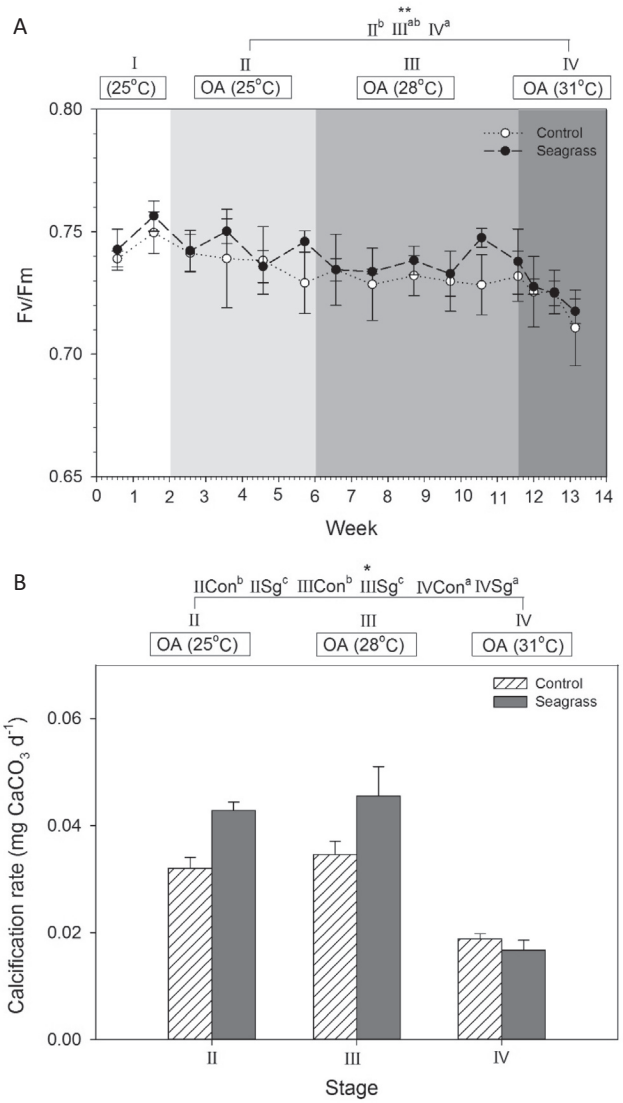

Fig. 4. (A) Maximum, dark-adapted yield of photosystem II (Fv/Fm) and (B) calcification rates of corals in response to ocean acidification (OA) and warming (mean ± SE; n = 3) in all four and the latter three experimental stages, respectively. Lowercase letters adjacent to experimental stage or treatment names at the top of each panel signify significant differences (Tukey's $p < 0.05$) between experimental stages and seagrass (Sg) and control (Con) mesocosms when the repeated measures ANOVAs (Supplementary Tables 6 and 7) (detected a significant overall effect of stage alone (a) or stage × treatment (b), respectively. In all cases, the group labeled "a" possessed the lowest value of the respective response variable.

by macroalgae (Beer, 1989) suggests that seagrasses are often limited by DIC in marine ecosystems (Invers et al., 2001). Some seagrass species have been reported to demonstrate higher photosynthetic efficiency (Fv/Fm), elevated leaf productivity, higher belowground biomass, and lower leaf nitrogen and chl-*a* content in response to the higher DIC concentrations associated with OA (Jiang et al., 2010, Repolho et al., 2017). Herein, although the Fv/Fm of *T. hemprichii* was not greatly affected by OA, shoot density and leaf growth rate both increased, which is consistent with results of prior studies (Palacios and Zimmerman, 2007; Andersson et al., 2011). Increasing the temperature to 28 °C or 31 °C under OA conditions further increased the shoot density, photosynthetic efficiency, and leaf growth rate of *T. hemprichii*. Higher leaf productivity of the seagrass *Zostera marina* in response to acidification was also observed (Palacios and Zimmerman, 2007). It is worth noting here that the faster decomposition rates of old and senesced seagrass leaves under higher temperatures (Huang et al., 2015) may have accounted for the higher concentrations of nitrite and nitrate in the seagrass mesocosms at 31 °C.

Upon acidification, the macroalga *D. bartayresiana* proliferated in all mesocosms. The congeneric *Dictyota dichotoma* was also dominant in high-pCO_2 vents off Castello Aragonese (Ischia Island, Italy) (Porzio et al., 2011). Many macroalgae can dampen the activity of HCO_3^--based carbon concentrating mechanisms (CCMs) and shift from use of HCO_3^- to CO_2 as their preferred carbon source in response to elevated CO_2 levels (Young and Gobler, 2016). Such a shift could explain why *D. bartayresiana* thrived under OA conditions in our mesocosms. Furthermore, the significantly lower phosphate concentrations in the controls relative to the seagrass mesocosms after increasing the pCO_2 and temperature may have been due to uptake by these macroalgae. Although the growth of *D. dichotoma* was presumably stimulated by OA herein, its growth rate sharply declined at 31 °C, and mortality was actually prevalent. Biber (2002) also found that macroalgal biomass decreases at this temperature in South Florida (similar latitude as Southern Taiwan).

The Fv/Fm of the coral *P. damicornis* did not decrease in response to OA, and its calcification rate was similar to that measured in the South China Sea at 29 °C (Jiang et al., 2017). *P. damicornis* is clearly not vulnerable to OA (as observed previously, Comeau et al., 2014), nor are the larvae (Putnam et al., 2013). However, upon increasing the temperature to 28 °C under OA conditions, Fv/Fm declined; the calcification rate, however, was unaffected until the temperature was raised to 31 °C for 13 days. In another mesocosm study carried out at the same facility, *P. damicornis* was found to actually bleach at 31.5 °C (Mayfield et al., 2013); our finding of diminished calcification at 31 °C under OA conditions herein is therefore unsurprising.

The calcification rate of *P. damicornis* in the seagrass mesocosms was significantly higher than in the controls at 25 °C and 28 °C under OA conditions. Prior studies (Lai et al., 2013, Hendriks et al., 2014) indicated that seagrasses may regulate local pH values and raise Ω_{Ar}, which could thereby enhance the calcification rates of nearby corals. However, pH and Ω_{Ar} were similar in the control and seagrass mesocosms. It is nevertheless possible that the sea-

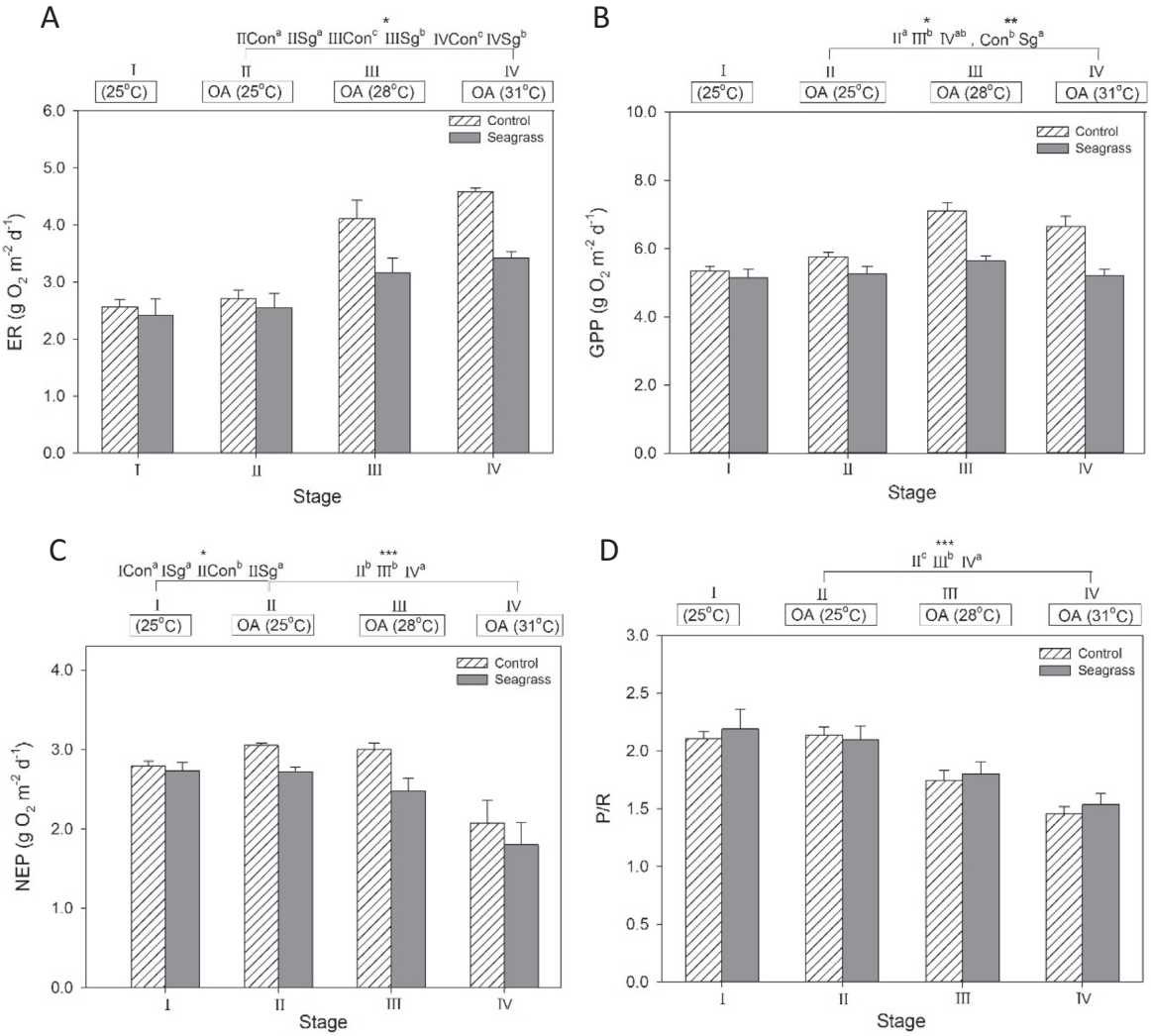

Fig. 5. Community metabolism parameters in control (Con) and seagrass (Sg) mesocosms (n = 3) at each of four experimental stages (mean ± SE). (A) Ecosystem respiration (ER) rate, (B) gross primary production (GPP), (C) net ecosystem metabolism (NEP), and (D) P/R ratio. Lowercase letters adjacent to experimental stage or treatment names at the top of each panel signify significant differences (Tukey's $p < 0.05$) between experimental stages (B-D), treatment (B), and/or the interaction of stage and treatment (A & C) when the repeated measures ANOVAs (Supplementary Tables 6 and 7) detected significant overall effects in the respective comparisons. In all cases, the group labeled "a" possessed the lowest value of the respective response variable.

grasses influenced coral calcification rates by other means, as discussed below.

Seagrasses compete with macroalgae for nutrients (Alexandre et al., 2017), which likely accounts for why macroalgal growth was lower in the seagrass mesocosms. Seagrass could also have reduced the degree of nutrient competition between macroalgae and *P. damicornis*, thereby accounting for (indirectly) the elevated coral calcification rates in the seagrass mesocosms. Corals can survive in oligotrophic systems because they can obtain nutrients from diverse sources, namely via the photosynthetic algae (family Symbiodinaceae) living in their tissues (Yonge, 1931; Jackson & Yellowlees, 1990; Ceh et al., 2013). However, autotrophic corals still rely on exogenous nutrients and therefore compete with primary producers such as macroalgae, periphyton, and seagrasses for nutrients in oligotrophic coral reef ecosystems. Our results showed that macroalgae are likely to bloom and rapidly consume nutrients in the water in response to elevated pCO_2 levels; this may account for why phosphate concentrations were barely detectable in the control, algae-enriched mesocosms. We surmise that this lack of phosphate could be another driver of the observed reduction in coral calcification in the seagrass-free control mesocosms given the importance of phosphate in coral photosynthesis (Annis and Cook, 2002). That being said, Symbiodinaceae dinoflagellates can obtain phosphate from dissolved organic sources, as well (Jackson and Yellowlees, 1990), and so this phosphate limitation hypothesis remains speculative.

The overall effects of seagrass on coral reef mesocosms can be further examined via assessment of the community metabolism data. In general, there is a positive relationship between algal biomass and GPP (Mulholland et al., 2001). Herein the GPP, NEP, and ER were all higher in the high-algal biomass controls under OA conditions, and the differences in GPP, NEP, and ER between the seagrass mesocosms and the controls became greater when the seawater temperature was increased to 28 °C. When the temperature reached 31 °C, the NEP in all mesocosms declined, although the NEP in the controls was still higher than in the seagrass mesocosms. The decline in NEP at 31 °C is likely due to reduced macroalgal biomass at this temperature, as has been documented in other studies of subtropical algae (Koch et al., 2013) (including the macroalga *Codium edule* in Nanwan Bay, Taiwan; Lin et al., 2007). Macroalgal degradation in our controls at 31 °C could also account for the increase in ER at this temperature.

5. Conclusions

The increase in DIC concentration in the seawater as a combined effect of OA and rising temperatures stimulated the growth of macroalgae, which may have preferentially exploited CO_2 as their major carbon source. However, the growth of macroalgae was less in the seagrass mesocosms than in the controls. OA did not have a significant effect on the coral *P. damicornis*. However, the calcification rates of the corals were higher in the seagrass mesocosms than in the controls, potentially as a result of competitive interactions between the seagrass and macroalgae. Macroalgal and coral growth both suffered at 31 °C under OA conditions. In contrast, seagrass shoot density, Fv/Fm, and leaf growth rate all increased with temperature. Consequently, the climate change factor-associated decline in NEP and ER in the seagrass mesocosms was less than in the controls, indicating that the presence of seagrass in the mesocosms can help stabilize (i.e., buffer) the system's metabolism in response to projected climate change stressors.

Author contributions

PJL and HJL conceived the ideas and designed the experiments; SJA collected and analyzed the data; HJL and ABM drafted the manuscript. All authors read and approved the final manuscript.

Declaration of Competing Interest

The authors declare that they have no known competing financial interests or personal relationships that could have appeared to influence the work reported in this paper.

Acknowledgments

This work was funded by 1) a research grant from the Ministry of Science and Technology (MOST) of Taiwan (MOST 105-2621-B-259-001 to PJL and HJL) and 2) the "Innovation and Development Center of Sustainable Agriculture" project administered by the "Featured Areas Research Center Program" within the Taiwanese Ministry of Education's "Higher Education Sprout Project." ABM was supported by a postdoctoral research fellowship from the Khaled bin Sultan Living Oceans Foundation during the time at which the research project was undertaken.

Appendix A. Supplementary data

Supplementary data associated with this article can be found online at https://doi.org/10.1016/j.scitotenv.2019.134464.

References

Albright, R., Caldeira, L., Hosfelt, J., Kwiatkowski, L., Maclaren, J.K., Mason, B.M., Nebuchina, Y., Ninokawa, A., Pongratz, J., Ricke, K.L., 2016. Reversal of ocean acidification enhances net coral reef calcification. Nature 531, 362.

Alexandre, A., Baeta, A., Engelen, A.H., Santos, R., 2017. Interactions between seagrasses and seaweeds during surge nitrogen acquisition determine interspecific competition. Sci. Rep. 7, 13651.

Andersson, A.J., Mackenzie, F.T., Gattuso, J.P., 2011. Effects of ocean acidification on benthic processes, organisms, and ecosystems. Ocean Acidification 8, 122–153.

Annis, E.R., Cook, C.B., 2002. Alkaline phosphatase activity in symbiotic dinoflagellates (zooxanthellae) as a biological indicator of environmental phosphate exposure. Mar. Ecol. Prog. Ser. 245, 11–20.

Anthony, K., Diaz-Pulido, G., Verlinden, N., Tilbrook, B., Andersson, A., 2013. Benthic buffers and boosters of ocean acidification on coral reefs. Biogeosciences 10, 4897–4909.

Baker, A.C., Glynn, P.W., Riegl, B., 2008. Climate change and coral reef bleaching: an ecological assessment of long-term impacts, recovery trends and future outlook. Estuarine, Coastal and Shelf Science 80, 435–471.

Beer, S., 1989. Photosynthesis and photorespiration of marine angiosperms. Aquat. Bot. 34, 153–166.

Bellwood, D.R., Hughes, T.P., Folke, C., Nyström, M., 2004. Confronting the coral reef crisis. Nature 429, 827.

Biber, P.D., 2002. The Effects of Environmental Stressors on the Dynamics of Three Functional Groups of Algae in *Thalassia testudinum* Habitats of Biscayne Bay, Florida: A Modeling Approach. Doctoral dissertation. University of Miami, Coral Gables, FL.

Bruno, J.F., Selig, E.R., 2007. Regional decline of coral cover in the Indo-Pacific: timing, extent, and subregional comparisons. PLoS ONE 2, e711.

Bruno, J.F., Valdivia, A., 2016. Coral reef degradation is not correlated with local human population density. Sci. Rep. 6, 29778.

Ceh, J., Kilburn, M.R., Cliff, J.B., Raina, J.-B., van Keulen, M., Bourne, D.G., 2013. Nutrient cycling in early coral life stages: *Pocillopora damicornis* larvae provide their algal symbiont (*Symbiodinium*) with nitrogen acquired from bacterial associates. Ecol. Evol. 3, 2393–2400.

Christianen, M.J., van Belzen, J., Herman, P.M., van Katwijk, M.M., Lamers, L.P., van Leent, P.J., Bouma, T.J., 2013. Low-canopy seagrass beds still provide important coastal protection services. PLoS ONE e62413.

Clarke, K.R., Warwick, R.M., 2001. Change in Marine Communities: An Approach to Statistical Analysis and Interpretation. PRIMER-E Ltd, Plymouth, UK.

Comeau, S., Carpenter, R., Nojiri, Y., Putnam, H., Sakai, K., Edmunds, P., 2014. Pacific-wide contrast highlights resistance of reef calcifiers to ocean acidification. Proc. R. Soc. London B: Biol. Sci. 281. 20141339.

Costanza, R., de Groot, R., Sutton, P., Van der Ploeg, S., Anderson, S.J., Kubiszewski, I., Farber, S., Turner, R.K., 2014. Changes in the global value of ecosystem services. Global Environ. Change 26, 152–158.

Davies, P.S., 1989. Short-term growth measurements of corals using an accurate buoyant weighing technique. Mar. Biol. 101, 389–395.

den Hartog, C., Kuo, J., 2007. Taxonomy and biogeography of seagrasses. In: Larkum, A.W.D., Orth, R.J., Duarte, C. (Eds.), Seagrasses: Biology, Ecology and Conservation. Springer, Dordrecht, Netherlands, pp. 1–23.

Diaz-Pulido, G., Anthony, K.R., Kline, D.I., Dove, S., Hoegh-Guldberg, O., 2012. Interactions between ocean acidification and warming on the mortality and dissolution of coralline algae. J. Phycol. 48, 32–39.

Donner, S.D., Rickbeil, G.J.M., Heron, S.F., 2017. A new, high-resolution global mass coral bleaching database. PLoS ONE e0175490.

Egea, L.G., Jiménez-Ramos, R., Vergara, J.J., Hernández, I., Brun, F.G., 2018. Interactive effect of temperature, acidification and ammonium enrichment on the seagrass *Cymodocea nodosa*. Mar. Pollut. Bull. 134, 14–26.

Egea, L.G., Jiménez-Ramos, R., Hernández, I., Brun, F.G., 2019. Effect of *In Situ* short–term temperature increase on carbon metabolism and dissolved organic carbon (DOC) fluxes in a community dominated by the seagrass *Cymodocea nodosa*. PLoS ONE 14 (1), e:0210386.

Flato, G., Marotzke, J., Abiodun, B., Braconnot, P., Chou, S.C., Collins, W.J., Cox, P., Driouech, F., Emori, S., Eyring, V., 2013. Evaluation of climate models. In: Stocker, T.F., Qin, D., Plattner, G.K., Tignor, M., Allen, S.K., Boschung, J., Nauels, A., Xia, Y., Bex, V., Midgley, P.M. (Eds.), Climate Change 2013: The Physical Science Basis. Contribution of Working Group I to the Fifth Assessment Report of the Intergovernmental Panel on Climate Change. Cambridge University Press, Cambridge, UK and New York, USA, pp. 741–866.

García, F.C., Bestion, E., Warfield, R., Yvon-Durocher, G., 2018. Changes in temperature alter the relationship between biodiversity and ecosystem functioning. Proc. Natl. Acad. Sci. U.S.A. 115 (43), 10989–10994.

Gardner, T.A., Côté, I.M., Gill, J.A., Grant, A., Watkinson, A.R., 2003. Long-term region-wide declines in Caribbean corals. Science 301, 958–960.

Gazeau, F., Parker, L.M., Comeau, S., Gattuso, J.P., O'Connor, W.A., Martin, S., Pörtner, H.O., Ross, P.M., 2013. Impacts of ocean acidification on marine shelled molluscs. Mar. Biol. 160, 2207–2245.

George, R., Gullström, M., Mangora, M.M., Mtolera, M.S.P., Björk, M., 2018. High midday temperature stress has stronger effects on biomass than on photosynthesis: a mesocosm experiment on four tropical seagrass species. Ecol. Evol. 8, 4508–4517.

Gillanders, B.M., 2007. Seagrasses, fish, and fisheries. In: Larkum, A.W.D., Orth, R.J., Duarte, C. (Eds.), Seagrasses: Biology, Ecology and Conservation. Springer, Dordrecht, Netherlands, pp. 503–505.

Helmuth, B., Babij, E., Duffy, E., Fauquier, D., Graham, M., Hollowed, A., Howard, J., Hutchins, D., Jewett, L., Knowlton, N., Kristiansen, T., Rowles, T., Sanford, E., Thornber, C., Wilson, C., 2013. Impacts of climate change on marine organisms. In: Griffis, R., Howard, J. (Eds.), Oceans and Marine Resources in a Changing Climate. Island Press, Washington, DC. NCA Regional Input Reports.

Hendriks, I.E., Olsen, Y., Ramajo, L., Basso, L., Steckbauer, A., Moore, T., Howard, J., Duarte, C., 2014. Photosynthetic activity buffers ocean acidification in seagrass meadows. Biogeosciences 11, 333.

Hoegh-Guldberg, O., Mumby, P.J., Hooten, A.J., Steneck, R.S., Greenfield, P., Gomez, E., Harvell, C.D., Sale, P.F., Edwards, A.J., Caldeira, K., 2007. Coral reefs under rapid climate change and ocean acidification. Science 318, 1737–1742.

Huang, Y.H., Hsiao, S.C., Lee, C.L., Chung, C.Y., Lin, H.J., 2015. Carbon budgets of multispecies seagrass beds at Dongsha Island in the South China Sea. Marine Environ. Res. 106, 92–102.

Invers, O., Zimmerman, R.C., Alberte, R.S., Pérez, M., Romero, J., 2001. Inorganic carbon sources for seagrass photosynthesis: an experimental evaluation of bicarbonate use in species inhabiting temperate waters. J. Exp. Mar. Biol. Ecol. 265, 203–217.

Jackson, A.E., Yellowlees, D., 1990. Phosphate uptake by zooxanthellae isolated from corals. Proc. R. Soc. London B: Biol. Sci. 242, 201–204.

Jiang, L., Sun, Y.F., Zhang, Y.Y., Zhou, G.W., Li, X.B., McCook, L.J., Lian, J.S., Lei, X.M., Liu, S., Cai, L., Qian, P.Y., Huang, H., 2017. Impact of diurnal temperature

fluctuations on larval settlement and growth of the reef coral *Pocillopora damicornis*. Biogeosciences 14 (24), 5741–5752.
Jiang, Z.J., Huang, X.P., Zhang, J.P., 2010. Effects of CO_2 enrichment on photosynthesis, growth, and biochemical composition of seagrass *Thalassia hemprichii* (Ehrenb.) Aschers. J. Integr. Plant Biol. 52, 904–913.
Katsikatsou, M., Anestis, A., Pörtner, H.O., Vratsistas, A., Aligizaki, K., Michaelidis, B., 2012. Field studies and projections of climate change effects on the bearded horse49 mussel *Modiolus barbatus* in the Gulf of Thermaikos, Greece. Mar. Ecol. Prog. Ser. 449, 183–196.
Kemp, W., Boynton, W., 1980. Influence of biological and physical processes on dissolved oxygen dynamics in an estuarine system: implications for measurement of community metabolism. Estuar. Coast. Mar. Sci. 11, 407–431.
Keppel, G., Wardell-Johnson, G.W., 2012. Refugia: keys to climate change management. Glob. Change Biol. 18, 2389–2391.
Knowlton, N., 2001. The future of coral reefs. Proc. Natl. Acad. Sci. 98, 5419–5425.
Koch, M., Bowes, G., Ross, C., Zhang, X.H., 2013. Climate change and ocean acidification effects on seagrasses and marine macroalgae. Glob. Change Biol. 19, 103–132.
Kroeker, K.J., Kordas, R.L., Crim, R., Hendriks, I.E., Ramajo, L., Singh, G.S., Duarte, C.M., Gattuso, J.P., 2013. Impacts of ocean acidification on marine organisms: quantifying sensitivities and interaction with warming. Glob. Change Biol. 19, 1884–1896.
Kurihara, H., Shirayama, Y., 2004. Effects of increased atmospheric CO_2 on sea urchin early development. Mar. Ecol. Prog. Ser. 274, 161–169.
Lai, S., Gillis, L., Mueller, C., Bouma, T., Guest, J., Last, K., Ziegler, A., Todd, P., 2013. First experimental evidence of corals feeding on seagrass matter. Coral Reefs 32, 1061–1064.
Lee, C.L., Huang, Y.H., Chen, C.H., Lin, H.J., 2016. Remote underwater video reveals grazing preferences and drift export in multispecies seagrass beds. J. Exp. Mar. Biol. Ecol. 476, 1–7.
Lee, C.L., Huang, Y.H., Chung, C.Y., Hsiao, S.C., Lin, H.J., 2015. Herbivory in multi-species, tropical seagrass beds. Mar. Ecol. Prog. Ser. 525, 65–80.
Lee, C.L., Wen, C.K.C., Huang, Y.H., Chung, C.Y., Lin, H.J., 2019. Ontogenetic habitat usage of juvenile carnivorous fish among seagrass-coral mosaic habitats. Diversity 11 (2), 25.
Lewis, E., Wallace, D., Allison, L.J., 1998. Program developed for CO2 system calculations. ORNL/CDIAC-105. Carbon Dioxide Information Analysis Center, Oak Ridge National Laboratory, US Department of Energy, Oak Ridge, Tennessee, USA.
Lin, H.J., Lee, C.L., Peng, S.E., Hung, M.C., Liu, P.J., Mayfield, A.B., 2018. The effects of El Niño-Southern Oscillation events on intertidal seagrass beds over a long-term timescale. Glob. Change Biol. 24, 4566–4580.
Lin, H.J., Wu, C.Y., Kao, S.J., Kao, W.Y., Meng, P.J., 2007. Mapping anthropogenic nitrogen through point sources in coral reefs using $\delta^{15}N$ in macroalgae. Mar. Ecol. Prog. Ser. 335, 95–109.
Liu, P.J., Hsin, M.C., Huang, Y.H., Fan, T.Y., Meng, P.J., Lu, C.C., Lin, H.J., 2015. Nutrient enrichment coupled with sedimentation favors sea anemones over corals. PLoS ONE e0125175.
Liu, P.J., Lin, S.M., Fan, T.Y., Meng, P.J., Shao, K.T., Lin, H.J., 2009. Rates of overgrowth by macroalgae and attack by sea anemones are greater for live coral than dead coral under conditions of nutrient enrichment. Limnol. Oceanogr. 54 (4), 1167–1175.
Liu, P.J., Meng, P.J., Liu, L.L., Wang, J.T., Leu, M.Y., 2012. Impacts of human activities on coral reef ecosystems of southern Taiwan: a long term study. Mar. Pollut. Bull. 64 (6), 1129–1135.
Lord, J.P., Barry, J.P., Graves, D., 2017. Impact of climate change on direct and indirect species interactions. Mar. Ecol. Prog. Ser. 571, 1–11.
Manzello, D.P., Enochs, I.C., Melo, N., Gledhill, D.K., Johns, E.M., 2012. Ocean acidification refugia of the Florida reef tract. PLoS ONE 7, e41715.
Marcarelli, A.M., Baxter, C.V., Mineau, M.M., Hall, R.O., 2011. Quantity and quality: unifying food web and ecosystem perspectives on the role of resource subsidies in freshwaters. Ecology 92, 1215–1225.
Mayfield, A.B., Chan, P.S., Putnam, H.M., Chen, C.S., Fan, T.Y., 2012. The effects of a variable temperature regime on the physiology of the reef-building coral *Seriatopora hystrix*: results from a laboratory-based reciprocal transplant. J. Exp. Biol. 215, 4183–4195.
Mayfield, A.B., Chen, M.N., Meng, P.J., Lin, H.J., Chen, C.S., Liu, P.J., 2013. The physiological response of the reef coral *Pocillopora damicornis* to elevated temperature: results from coral reef mesocosm experiments in Southern Taiwan. Mar. Environ. Res. 86, 1–11.
Moreno-Marín, F., Vergara, J.J., Pérez-Llorens, J.L., Pedersen, M.F., Brun, F.G., 2016. Interaction between ammonium toxicity and green tide development over seagrass meadows: a laboratory study. PLoS ONE 11, (4) e0152971.
Mulholland, P., Fellows, C., Tank, J., Grimm, N., Webster, J., Hamilton, S., Marti, E., Ashkenas, L., Bowden, W., Dodds, W., 2001. Inter-biome comparison of factors controlling stream metabolism. Freshw. Biol. 46, 1503–1517.
Nordlund, L.M., Jackson, E.L., Nakaoka, M., Samper-Villarreal, J., Beca-Carretero, P., Creed, J.C., 2017. Seagrass ecosystem services–What's next? Mar. Pollut. Bull. 134, 145–151.
Odum, H.T., 1956. Primary production in flowing waters. Limnol. Oceanogr. 1, 102–117.
Pai, S.C., Riley, J., 1994. Determination of nitrate in the presence of nitrite in natural waters by flow injection analysis with a non-quantitative on-line cadmium reductor. Int. J. Environ. Anal. Chem. 57, 263–277.
Palacios, S.L., Zimmerman, R.C., 2007. Response of eelgrass *Zostera marina* to CO_2 enrichment: possible impacts of climate change and potential for remediation of coastal habitats. Mar. Ecol. Prog. Ser. 344, 1–13.
Poloczanska, E.S., Brown, C.J., Sydeman, W.J., Kiessling, W., Schoeman, D.S., Moore, P. J., Brander, K., Bruno, J.F., Buckley, L.B., Burrows, M.T., 2013. Global imprint of climate change on marine life. Nat. Clim. Change 3, 919–925.
Porzio, L., Buia, M.C., Hall-Spencer, J.M., 2011. Effects of ocean acidification on macroalgal communities. J. Exp. Mar. Biol. Ecol. 400, 278–287.
Putnam, H.M., Mayfield, A.B., Fan, T.Y., Chen, C.S., Gates, R.D., 2013. The physiological and molecular responses of larvae from the reef-building coral *Pocillopora damicornis* exposed to near-future increases in temperature and pCO_2. Mar. Biol. 160, 2157–2173.
Repolho, T., Duarte, B., Dionísio, G., Paula, J.R., Lopes, A.R., Rosa, I.C., Grilo, T.F., Caçador, I., Calado, R., Rosa, R., 2017. Seagrass ecophysiological performance under ocean warming and acidification. Sci. Rep. 7, 41443.
Riddle, D., 2013. Aquarium equipment: PAR meters and LEDs – how accurate are the measurements? A comparison of three meters and Lux to PAR conversion factors for LEDs. Retrieved May 10, 2018, from https://www.advancedaquarist.com/.
Sand-Jensen, K., Gordon, D.M., 1984. Differential ability of marine and freshwater macrophytes to utilize HCO_3^- and CO_2. Mar. Biol. 80, 247–253.
Shalders, T.C., Saunders, B.J., Bennett, S., Parker, J.R.C., Harvey, E.S., 2018. Potential climate-mediated changes to the distribution and density of pomacentrid reef fishes in south-western Australia. Mar. Ecol. Prog. Ser. 604, 223–235.
Short, F.T., Duarte, C.M., 2001. Methods for the measurement of seagrass growth and production. Global Seagrass Res. Methods 2001, 155–198.
Stocker, T.F., Qin, D., Plattner, G.K., Alexander, L.V., Allen, S.K., Bindoff, N.L., Bréon, F. M., Church, J.A., Cubasch, U., Emori, S., 2013. Technical summary. In: Field, C.B., Barros, V.R., Dokken, D.J., Mach, K.J., Mastrandrea, M.D., Bilir, T.E., Chatterjee, M., Ebi, K.L., Estrada, Y.O., Genova, R.C., Girma, B., Kissel, E.S., Levy, A.N., MacCracken, S., Mastrandrea, P.R., White, L.L. (Eds.), Climate Change 2013: The Physical Science Basis. Contribution of Working Group I to the Fifth Assessment Report of the Intergovernmental Panel on Climate Change. Cambridge University Press, Cambridge, UK and New York, USA, pp. 33–115.
Strickland, J.D., Parsons, T.R., 1972. A Practical Handbook of Seawater Analysis. Fisheries Research Board of Canada, Ottawa, Canada.
Thorp, J.H., Delong, M.D., 2002. Dominance of autochthonous autotrophic carbon in food webs of heterotrophic rivers. Oikos 96, 543–550.
van de Koppel, J., van der Heide, T., Altieri, A.H., Eriksson, B.K., Bouma, T.J., Olff, H., Silliman, B.R., 2015. Long-distance interactions regulate the structure and resilience of coastal ecosystems. Annu. Rev. Mar. Sci. 7, 139–158.
van Vuuren, D.P., Edmonds, J., Kainuma, M., Riahi, K., Thomson, A., Hibbard, K., Hurtt, G.C., Kram, T., Krey, V., Lamarque, J.F., 2011. The representative concentration pathways: an overview. Clim. Change 109, 5.
Walther, K., Sartoris, F.J., Bock, C., Pörtner, H.O., 2009. Impact of anthropogenic ocean acidification on thermal tolerance of the spider crab *Hyas araneus*. Biogeosciences 6, 2207–2215.
Yonge, C., 1931. Studies on the physiology of corals. IV. The structure, distribution and physiology of the zooxanthellae. Great Barrier Reef Expedition 1928–29. Scientific Rep. British Museum 1, 135–176.
Young, C.S., Gobler, C.J., 2016. Ocean acidification accelerates the growth of two bloom-forming macroalgae. PLoS ONE e0155152.